Optimal Sizing and Placement of Smart Grid Enabling Technologies for Maximizing Renewable Integration

Sérgio F. Santos[a], Desta Z. Fitiwi[a], M. Shafie-khah[a,b], Abebe W. Bizuayehu[a], and João P. S. Catalão[a,c,d,*]

[a] University of Beira Interior, R. Fonte do Lameiro, 6201-001 Covilhã, Portugal
[b] University of Salerno, Via Giovanni Paolo II, 132, Fisciano (SA), 84084 Salerno, Italy
[c] Faculty of Engineering of the University of Porto, R. Dr. Roberto Frias, 4200-465 Porto, Portugal
[d] INESC-ID, Inst. Super. Tecn., University of Lisbon, Av. Rovisco Pais, 1, 1049-001 Lisbon, Portugal

* E-mail of the corresponding author: catalao@ubi.pt

TABLE OF CONTENTS

ABSTRACT

This work presents a new integrated multi-stage and stochastic mathematical model, which is developed to support the decision-making process related to the expansion planning of distribution network systems (DNS) for integrating large-scale distributed "clean" energy sources. The developed model, formulated from the distribution system operator's point of view, determines the optimal sizing, time and placement of distributed energy technologies (renewables, in particular) as well as that of energy storage systems (ESS) and compensators in distribution networks. The ultimate goal of this optimization work is to maximize the size of distributed generation (DG) power absorbed by the system while maintaining the power quality and stability at the required/standard levels at a minimum cost possible. The model, formulated as a mixed integer linear programming (MILP) optimization, employs a linearized alternating current (AC) network model which captures well the inherent characteristics of power network systems, and balances accuracy with computational burden. The standard IEEE 41-bus distribution system is used to test the developed model and carry out the required analysis from the standpoint of the objectives set.

The results of the case study show that the integration of ESS and compensators helps to significantly increase the size of variable generation (wind and solar) in the system. For the case study, a total of 10 MW demand wind and solar power has been added to the system. One can put this into perspective with the peak load 4.635 MW in the system. This means it has been possible to integrate RES power more than twice the peak demand in the base case. It has been demonstrated that the joint planning of DGs, compensators and ESS, proposed in this work, brings about significant improvements to the system such as reduction of losses, cost of electricity and emissions, voltage support and many more others.

The expansion planning model proposed here can be considered as a major leap forward towards developing controllable grids, which support large-scale integration of RESs (as opposed to the conventional "fit and forget" approach). It can also be a handy tool to speed up the integration of more RESs until smart grids are materialized in the future.

1. INTRODUCTION

Nowadays, the issue of integrating DGs (RESs, in particular) is globally gaining momentum because of several techno-economic and environmental factors. Since recent years, the size of DGs integrated into distribution systems has been increasing. And, this trend is more likely to continue in the years to come because it is now widely accepted that DGs bring wide-range benefits to the system, in general. However, given the current set-up of distribution networks (which are generally passive), large-scale DG integration is not technically possible because this brings about tremendous challenges to the system operation, especially in undermining the power system quality and stability. Such challenges/ limitations are expected to be alleviated when distribution networks undergo the anticipated evolutionary process from passive to active networks or smart grids. This transition is expected to result in a system that is adequately equipped with appropriate technologies, state-of-the-art solutions and a new operational philosophy that is totally different from the current 'fit and forget' approach. And, this is expected to offer sufficient flexibility and control mechanism in the system. Nevertheless, the process is not straightforward as it demands exceptionally huge investments in smart-grid technologies and concepts to fully automate the system, and this should be accompanied by a new operational philosophy. Therefore, if not impossible, the whole transformation process i.e. the transformation of current distribution systems to full-scale smart-grids might be very slow, and its realization might take several decades.

However, given the techno-economic factors and global concerns about environmental issues, the integration of RESs cannot be postponed. It is likely that the integration of DGs in distribution systems will go ahead along with smart-grid enabling technologies that have the capability to alleviate the negative consequences of large-scale integration of DGs. In other words, in order to facilitate (speed up) the much-needed transformation of conventional (passive) DNSs and support large-scale RES integration, different smart-grid enabling technologies such as reactive power compensators, advanced switching and storage devices are expected to be massively deployed in the near term. To this end, developing strategies, methods and tools to maximize the penetration level of DGs (particularly, RESs) has become very crucial to guide such a complex decision-making process. In this respect, this work focuses on the development of multi-stage mathematical models to determine the optimal sizing, time and placement of energy storage systems and compensators as well as that of RESs in distribution networks. The ultimate goal of this optimization work is to maximize the DG power absorbed by the system at a minimum cost while maintaining the power quality and stability at the required/standard levels.

2. State-of-the-art Literature Review

Reducing fossil fuel dependence and mitigating climate change has led to increased pressure to change the current generation paradigm. It is expected that CO_2 emissions will increase from approximately 31 billion metric tons to 36 billion metric tons in 2020, reaching 45 billion metric tons by mid-2040 [1], an increase of 46%. Other associated concerns are an increase in global average temperature from 1 to 5 ºC by the year 2100, increasing the average level of the sea water [2]. Global population will also increase, expected to be 9.6 billion in 2050, along with an increase in energy consumption by 56% between 2010 and 2040 [1]. The compounded effect of all these problems and challenges is triggering a policy shift all over the world, especially when it comes to energy production. Integration of distributed generation (DG), particularly, renewable energy sources (RESs), in electric distribution network systems is gaining momentum. It is highly expected that large-scale DG integration will be one of the solutions capable of mitigating the aforementioned problems and overcoming the challenges. Because of this, Governments of various nations have introduced targets to achieve large-scale integration of DGs. In particular, in the European Union (EU), which strongly advocates the importance of integrating DGs (especially, renewables), that is expected to grow by 20% until 2020 and 50% of energy consumption by 2050.

Power distribution networks form a critical base to system reliability, power quality and also energy cost [3,4]. One way of making the distribution system "less critical", is through the integration of DG systems that are small power sources connected near the end users. DG offers a more environmentally friendly option through great opportunities with renewable-enabling technologies such as wind, photovoltaic, biomass, etc. RESs are abundant in nature, which leads to the attraction of the large-scale power generation sector. Nevertheless, there is no rule or partial rule on the DG unit's connection; typically, these are connected at the end of radial feeder systems or nodes with greater load on the distribution system. The size of DG can vary from a few kW to several MW depending also on the voltage system level to which they are connected. The optimal planning of the DG unit's placement and sizing will become extremely important for energy producers, consumers and network operators in technical and economic terms in the near future. There are many studies in the literature on this topic, yet most of them only consider the optimal location of a single DG unit or do not consider simultaneously positioning and sizing units, mainly due to the high dispatch unpredictability of these. The increase in DGs penetration increases the uncertainty and the fluctuations of the system production. If the placement and proper sizing is not taken into account, the benefits of DG integration can be lost in efficiency losses, increasing the electricity cost and leading to energy losses.

Another major concern with the wide DG penetration is system reliability. In this paradigm, the use of ESS has been seen as one of the viable options to mitigate the aforementioned concerns. The penetration of distributed systems can result in the degradation of power quality, particularly in cases of slightly meshed networks [5] or microgrids. Electricity production fluctuations can create voltage oscillations in a frequency range between 1–10 Hz. One possible approach for reducing voltage fluctuations in microgrids or slightly meshed networks is through a specific frequency damping; yet the use of ESS is required for a range of frequencies. Several ESS technologies are emerging, especially for demanding cases of charge and quick dispatch cycles. However, the smooth integration of energy storage systems in the grid requires power electronics based interfaces. Normally, the ESS is connected at the renewable energy source coupling point. To perform energy smoothing, a comparison between the attenuation of fast power variation and regulation of the state of charge should be made. The latter is necessary to maximize the ability to deliver energy [6].

The DG allocation and sizing subject have received special interest from researchers in recent years as shown in [7], a review on the subject until 2013. In [7] and [8], an analysis of several innovative techniques used on the DG impact investigation in the electrical system is presented. Most of these techniques analyze the distribution system to determine rules that can be used for DG integration [9–13]. Important issues related to the connection of DG units are the network topology, DG capacity and suitable location; because, each bus in the system has an optimal level of DG integration. And, if the value surpasses this level, system losses can increase [14], [15]. There are many ways proposed to formulate and analyze the optimal allocation of multiple DG units in a radial or meshed network.

Recently, several methods have been proposed for planning and operation or in some cases for both location and sizing of DGs in the distribution system. In general, these methods can be classified as heuristic based [16–31], numerical based [32–39] and analytical based [40], [41] methods.

Heuristic based methods apply advanced artificial intelligence algorithms, such as Genetic Algorithms (GA) [16–19], Particle Swarm Optimization (PSO) [20–24], Harmony Search (HS) [25], [26] and Big Bang Crunch (BBC) [27–29]. In [16], GA is used to solve the expansion planning problem considering DG, uncertainties and reliability in normal operating conditions. Another approach widely used with GA is the non-dominated sorting genetic algorithm (NSGA-II) [17]. Another work that also uses the NSGA-II is [18], where multi-objective integration approach of DG and ESS in distribution systems. In [19] is presented a comparison between Mixed-Integer Programming (MIP) and GA Methods for DG Planning. PSO is another method used, whether in its original version or an improved version such as multi-objective particle swarm optimization (MPSO) [20] or hybrid multi-objective particle swarm optimization (HMOPSO) [21]. In [22], a PSO algorithm was used to solve a distribution system expansion planning problem, considering ESSs and DG systems. The work presented in [23] investigated the impact of ESSs in the distribution system multistage expansion planning problem, being formulated as an optimization problem and solved using PSO. This work indicates a positive impact of the ESS on the performance and costs associated with the network. A multi-objective particle swarm optimization (MOPSO) approach is proposed in [21], to minimize the power system cost and to improve the system voltage profiles by searching siting and sizing of storage units under consideration of uncertainties in wind power production. Authors in [24] presented a new approach to optimize the allocation and sizing of several DG units based on the maximization of loading systems using hybrid particle swarm optimization (HPSO). HS is another heuristic based methodology widely used, as in [25], which minimizes energy losses by distribution systems reconfiguration in the presence of DG. Another work that uses HS is [26] where an Improved Multi-Objective Harmony Search (IMOHS) is used in order to obtain the optimal location of DGs in the distribution system. One method that has been commonly used is the Big Bang Crunch (BBC), which is a method based on the evolution of the universe that has been applied to solving the problems of DG placement and sizing in the distribution system. In particular, [27], where the Hybrid Big Bang (HBBC), is used for reconfiguration and optimal allocation of DG in the distribution system. The work in [28] proposes an algorithm for modelling stochastically renewable based DGs with the purpose of planning an unbalanced distribution network; the BBC algorithm is used to perform optimal DG placement. Authors in [29] use a modified BBC method to deal with the optimization problems incorporating multiple distributed generators for the sake of power, as well as energy loss minimization in balanced/unbalanced distribution systems. Two other algorithms that also have been used are Water Drop (WD) and Fireworks Algorithm (FW). The intelligent algorithm WD [30] is used for the DG allocation and sizing, with the goal of minimizing energy losses and improving the voltage profile. In [31], authors present DG optimal allocation and distribution system reconfiguration, in order to minimize energy losses and voltage stability using FW.

Numerical methods are algorithms that seek numerical results for different problems in particular to the problem in question. Some of the most recently works use nonlinear mixed integer programming (MINLP) [32–34], mixed integer linear programming (MILP) [35], [36], quadratic programming (QP) [37] and optimal power flow (OPF) [38]. Reference [32] shows the allocation of DG using a decision made by the system approach planner (DMSP) based on the utilities and customer aspects under a deregulated environment; the problem uses OPFs formulation and is solved with MINLP. In [33], one MINLP algorithm is presented to solve the optimal placement and sizing of DG with the goal of improving the voltage stability margin in the distribution system. A planning MINLP algorithm on a statistical basis is proposed in [34] to determine the optimal generation mix of different renewable DG unit types in an annual base to minimizing the energy losses in the distribution system. One other approach within the numerical methods is through MILP algorithms. The authors of [35] focus on the problem in the optimal configuration/design of distributed resources, produced outside of buildings and sent to these through the distribution networks. The model provides the simultaneous optimal locations (i.e. the place of production) as well as synthesizes (type, capacity and number of equipment) and operational strategies for the entire system through a MILP model. A MILP algorithm is also used in [36], in a two-stage stochastic model multi-period. The work in [37] presents a simultaneous optimization of ESS and DG in microgrids, and is solved by a not sequential quadratic programming algorithm. The optimum installation of DG technologies to minimize energy losses in the distribution system is presented in [38], using an efficient analytical (EA) algorithm integrated with OPF algorithm, a new method EA/OPF. The DG unit planning in the distribution system is presented in [39] using a hierarchical agglomerative clustering algorithm (HACA).

The exhaustive search methods are based on the search for the optimal DG location for a given DG size under different load models. Therefore, these methods fail to represent accurately the DG optimization problem behavior involving two continuous variables, both for optimum DG size and optimal DG location. In [40], authors present one technique with a probabilistic basis for determining the capacity and optimal placement of wind DG units to minimize energy loss in the distribution system. A sensitivity algorithm is presented in [41] for DG placement and sizing in the network.

Despite the many studies in the literature on areas related to DG placement and sizing problem, most of them only consider the optimal location of a single DG unit, mostly of conventional DGs. The simultaneous consideration of the placement, timing and sizing of DG units (especially RESs), along with the placement, timing and sizing of smart-grid enabling technologies, seems to be far from being addressed in the literature. The increase in RES-based DG penetration increases the uncertainty and the fluctuations of the system production. If the placement and proper sizing is not taken into account, the benefits of DG integration may not be exploited; instead, this may result in the degradation of system efficiency, increased cost of electricity and energy losses. Another major concern with the wide-range DG penetration is system reliability. However, the simultaneous investment planning of DGs, ESSs and compensators is expected to significantly alleviate these challenges and increase the penetration level of RES-based DGs.

3. OBJECTIVES

The main objectives of this work are:

- To develop a new joint multi-stage mathematical optimization model considering smart-grid enabling technologies such as ESS, compensators, and network switching and/or expansion to support DG integration.
- To determine the optimal sizing, time and placement of energy storage systems and compensators as well as that of RESs in distribution networks. The ultimate goal of this optimization work is to maximize the DG power absorbed by the system at a minimum cost while maintaining the power quality and stability at the required/standard levels.
- To carry out case studies and test the developed model.
  To analyze simulation results and disseminate research outcomes.

4. MATHEMATICAL FORMULATION OF THE PROBLEM

4.1. Introduction

As mentioned earlier, the work here develops an integrated optimization model that simultaneously finds the optimal locations and sizes of installed DG power (particularly, focusing on wind and solar), energy storage systems and capacitor banks. The optimal deployment of the aforementioned enabling technologies should inherently meet the goal of maximizing the renewable power integrated/absorbed into the system. The entire model is formulated as a stochastic mixed integer linear programming (SMILP) optimization. In addition, instead of the customary DC network models, a linearized AC model is used in the formulation to better capture the inherent characteristics of the network system.

4.2. Objective Function

As mentioned earlier, the objective of this work is to maximize RES integration in DNS from the system perspective (or, from the Distribution System Operators' point of view) by optimally deploying different smart-grid enabling technologies at a minimum cost. Here, it is assumed that the DSO owns some generation sources and ESSs.

The resulting problem is formulated as a multi-objective stochastic MILP with two objectives: maximization of integrated RES energy as in (1a) and overall cost minimization (1b). The problem can be considered as a minimax optimization. However, the first objective can be considered to be redundant if the cost of RES energy (tariff) is very small or the RESs is prioritized when carrying out the dispatch in the system (as it is the case in most power systems). This is because, in such cases, the generated RES power will be fully integrated as far as this maintains the power quality and stability at the required/standard levels. In this work, only (1b) is considered. The objective function in (1b) is composed of Net Present Value (NPV) of five cost terms each weighted by a certain relevance factor $\alpha_j; \forall j \in \{1,2,\ldots,5\}$. Note that, in this work, all cost terms are assumed to be equally important; hence, these factors are set to 1. However, depending on the relative importance of the considered costs, different weights can be adopted in the objective function. The first term in (1b), $TInvC$, represents the total investment costs under the assumption of perpetual planning horizon [42]. In other words, "the investment cost is amortized in annual installments throughout the lifetime of the installed component", as is done in [43]. Here, the total investment cost is the sum of investment costs of new and existing DGs, feeders, energy storage system and capacitor banks, as in (2).

The second term, TMC, in (1b) denotes the total maintenance costs, which is given by the sum of individual maintenance costs of new and existing DGs, feeders, energy storage system and capacitor banks in the system at each stage and the corresponding costs incurred after the last planning stage, as in (3). Note that the latter costs depend on the maintenance costs of the last planning stage. Here, a perpetual planning horizon is assumed. The third term TEC in (1b) refers to the total cost of energy in the system, which is the sum of the cost of power produced by new and existing DGs, purchased from upstream and supplied by energy storage system at each stage as in (4). Equation (4) also includes the total energy costs incurred after the last planning stage under a perpetual planning horizon. These depend on the energy costs of the last planning stage. The fourth term $TENSC$ represents the total cost of unserved power in the system and is calculated as in (5). The last term $TImiC$ gathers the total emission costs in the system, given by the sum of emission costs for the existing and new DGs as well that of power purchased from the grid at the substations.

$$Maximize\ Total\ RES\_Energy = \sum_{t\epsilon\Omega^t}\sum_{s\epsilon\Omega^s}\rho_s\sum_{w\epsilon\Omega^w}\pi_w\sum_{g\epsilon\Omega^{RES}}\sum_{i\epsilon\Omega^i}(P^N_{g,i,s,w,t}) \quad (1a)$$

$$Minimize\ TC = \alpha_1 * TInvC + \alpha_2 * TMC + \alpha_3 * TEC + \alpha_4 * TENSC + \alpha_5 * TImiC \quad (1b)$$

$$TInvC = \underbrace{\sum_{t\epsilon\Omega^t}\frac{(1+r)^{-t}}{r}(InvC^{DG}_t + InvC^{LN}_t + InvC^{ES}_t + InvC^{CAP}_t)}_{NPV\ of\ investment\ cost} \quad (2)$$

$$TMC = \underbrace{\sum_{t\epsilon\Omega^t}(1+r)^{-t}\ (MC^{DG}_t + MC^{LN}_t + MC^{ES}_t + MC^{Cap}_t)}_{NPV\ of\ maintenance\ costs} + \underbrace{\frac{(1+r)^{-T}}{r}(MC^{DG}_T + MC^{LN}_T + MC^{ES}_T + MC^{Cap}_T)}_{NPV\ maintenance\ costs\ incured\ after\ stage\ T} \quad (3)$$

$$TEC = \underbrace{\sum_{t\epsilon\Omega^t}(1+r)^{-t}\ (EC^{DG}_t + EC^{ES}_t + EC^{SS}_t)}_{NPV\ of\ operation\ costs} + \underbrace{\frac{(1+r)^{-T}}{r}(EC^{DG}_T + EC^{ES}_T + EC^{SS}_T)}_{NPV\ operation\ costs\ incured\ after\ stage\ T} \quad (4)$$

$$TENSC = \underbrace{\sum_{t\epsilon\Omega^t}(1+r)^{-t}\ ENSC_t}_{NPV\ of\ reliability\ costs} + \underbrace{\frac{(1+r)^{-T}}{r}ENSC_T}_{NPV\ reliability\ costs\ incured\ after\ stage\ T} \quad (5)$$

$$TEmiC = \underbrace{\sum_{t\epsilon\Omega^t}(1+r)^{-t}\ (EmiC^{DG}_t + EmiC^{SS}_t)}_{NPV\ emission\ costs} + \underbrace{\frac{(1+r)^{-T}}{r}(EmiC^{DG}_T + EmiC^{SS}_T)}_{NPV\ emission\ costs\ incured\ after\ stage\ T} \quad (6)$$

The individual cost components in (2)—(6) are computed by the following expressions. Equations (7)—(10) represent the investment costs of DGs, feeders, energy storage system and capacitor banks, respectively. Notice that all investment costs are weighted by the capital recovery factor, $\frac{r(1+r)^{LT}}{(1+r)^{LT}-1}$. The formulations in (7)—(10) ensure that the investment cost of each component added to the system is considered only once in the summation. For example, suppose an investment in a particular feeder k is made in the second year of a three-year planning horizon. This means that the feeder should be available for utilization after the second year. Hence, the binary variable associated to this feeder will be 1 after the second year while zero otherwise i.e. $x_{k,t} = \{0,1,1\}$. In this particular case, only the difference $(x_{k,2} - x_{k,1})$ equals 1, implying that the investment cost is considered only once. It should be noted that this works regardless of the type of the investment variables. Suppose instead of only binary, $x_{k,t}$ is allowed to have integer values. Assume the optimal solution is $x_{k,t} = \{0,1,2\}$. In this case, the corresponding difference $(x_{k,t} - x_{k,t-1})$ becomes $\{0,1,1\}$, indicating that the investment costs of only those components added at each stage are considered in the summation. Equation (11) stands for the maintenance costs of new and existing DGs at each time stage. The maintenance cost of a new/existing feeder is included only when its corresponding investment/utilization variable is different from zero. Similarly, the maintenance costs of new and existing feeders at each stage are given by equation (12). Equations (13) and (14) are related to the maintenance costs at each stage of energy storage and capacitor banks, respectively.

$$InvC_t^{DG} = \sum_{g\epsilon\Omega^g}\sum_{i\epsilon\Omega^i}\frac{r(1+r)^{LT_g}}{(1+r)^{LT_g}-1}IC_{g,i}(x_{g,i,t} - x_{g,i,t-1}) \text{ ; } where\ x_{g,i,0} = 0 \tag{7}$$

$$InvC_t^{LN} = \sum_{k\epsilon\Omega^\ell}\frac{r(1+r)^{LT_k}}{(1+r)^{LT_k}-1}IC_k(x_{k,t} - x_{k,t-1}) \text{ ; } where\ x_{k,0} = 0 \tag{8}$$

$$InvC_t^{ES} = \sum_{es\epsilon\Omega^{es}}\sum_{i\epsilon\Omega^i}\frac{r(1+r)^{LT_{es}}}{(1+r)^{LT_{es}}-1}IC_{es}(x_{es,i,t} - x_{es,i,t-1}) \text{ ; } where\ x_{es,i,0} = 0 \tag{9}$$

$$InvC_t^{CAP} = \sum_{c\epsilon\Omega^c}\sum_{i\epsilon\Omega^i}\frac{r(1+r)^{LT_c}}{(1+r)^{LT_c}-1}IC_c(x_{c,i,t} - x_{c,i,t-1}) \text{ ; } where\ x_{c,i,0} = 0 \tag{10}$$

$$MC_t^{DG} = \sum_{g\epsilon\Omega^g}\sum_{i\epsilon\Omega^i}MC_g^N\, x_{g,i,t} + \sum_{g\epsilon\Omega^g}\sum_{i\epsilon\Omega^i}MC_g^E\, u_{g,i,t} \tag{11}$$

$$MC_t^{LN} = \sum_{k\epsilon\Omega^{e\ell}}MC_k^E\, u_{k,t} + \sum_{k\epsilon\Omega^{n\ell}}MC_k^N x_{k,t} \tag{12}$$

$$MC_t^{ES} = \sum_{es\epsilon\Omega^{es}}\sum_{i\epsilon\Omega^i}MC_{es}x_{es,i,t} \tag{13}$$

$$MC_t^{Cap} = \sum_{c\epsilon\Omega^c}\sum_{i\epsilon\Omega^i}MC_c x_{c,i,t} \tag{14}$$

The total cost of power produced by new and existing DGs is given by equation (15). Note that these costs depend on the amount of power generated at each scenario, snapshot and stage. Therefore, these costs represent the expected costs of operation. Similarly, equations (16) and (17) respectively account for the expected costs of energy supplied by the energy storage system, and that purchased from upstream (i.e. transmission grid). The penalty for the unserved power, given by (18), is also dependent on the scenarios, snapshots and time stages. Equation (18) therefore gives the expected cost of unserved energy in the system. The expected emission costs of power generated by new and existing DGs are given by (19)-(21), and that of energy purchased from the grid is calculated using (22). Note that, for the sake of simplicity, a linear emission cost function is assumed here. In reality, the emission cost function is highly nonlinear and nonconvex, as in [44].

$$EC_t^{DG} = \sum_{s\epsilon\Omega^s}\rho_s\sum_{w\epsilon\Omega^w}\pi_w\sum_{g\epsilon\Omega^g}\sum_{i\epsilon\Omega^i}(OC_{g,i,s,w,t}^N P_{g,i,s,w,t}^N + OC_{g,i,s,w,t}^E P_{g,i,s,w,t}^E) \tag{15}$$

$$EC_t^{ES} = \sum_{s\epsilon\Omega^s} \rho_s \sum_{w\epsilon\Omega^w} \pi_w \sum_{c\epsilon\Omega^c} \sum_{i\epsilon\Omega^i} \gamma_{es,i,s,w,t}^{dch} P_{es,i,s,w,t}^{dch} \tag{16}$$

$$EC_t^{SS} = \sum_{s\epsilon\Omega^s} \rho_s \sum_{w\epsilon\Omega^w} \pi_w \sum_{\varsigma,\Omega^\varsigma} \sigma_{\varsigma,s,w,t} P_{\varsigma,s,w,t}^{SS} \tag{17}$$

$$ENSC_t = \sum_{s\epsilon\Omega^s} \rho_s \sum_{w\epsilon\Omega^w} \sum_{i\epsilon\Omega^i} \pi_w \upsilon_{s,w,t} \delta_{i,s,w,t} \tag{18}$$

$$EmiC_t^{DG} = EmiC_t^N + EmiC_t^E \tag{19}$$

$$EmiC_t^N = \sum_{s\epsilon\Omega^s} \rho_s \sum_{w\epsilon\Omega^w} \pi_w \sum_{g\epsilon\Omega^g} \sum_{i\epsilon\Omega^i} \lambda_{s,w,t}^{CO_2e} ER_g^N P_{g,i,s,w,t}^N \tag{20}$$

$$EmiC_t^E = \sum_{s\epsilon\Omega^s} \rho_s \sum_{w\epsilon\Omega^w} \pi_w \sum_{g\epsilon\Omega^g} \sum_{i\epsilon\Omega^i} \lambda_{s,w,t}^{CO_2e} ER_g^E P_{g,i,s,w,t}^E \tag{21}$$

$$EmiC_t^{SS} = \sum_{s\epsilon\Omega^s} \rho_s \sum_{w\epsilon\Omega^w} \pi_w \sum_{\varsigma\epsilon\Omega^\varsigma} \lambda_{s,w,t}^{CO_2e} ER_\varsigma^{SS} P_{\varsigma,s,w,t}^{SS} \tag{22}$$

4.3. Constraints

3.3.1. Kirchhoff's voltage law

The customary AC power flow equations, given by (23) and (24), are highly non-linear and non-convex. Understandably, using these flow expressions in power system planning applications is increasingly difficult. Because of this, Equations (23) and (24) are often linearized by considering two practical assumptions. The first assumption is concerning the bus voltage magnitudes, which in distribution systems are expected to be close to the nominal value V_{nom}. The second assumption is in relation to the voltage angle difference θ_k across a line which is practically small, leading to the trigonometric approximations $sin\theta_k \approx \theta_k$ and $cos\theta_k \approx 1$. Note that this assumption is valid in distribution systems, where the active power flow dominates the total apparent power in lines. Furthermore, the voltage magnitude at bus i can be expressed as the sum of the nominal voltage and a small deviation ΔV_i, as in (25).

$$P_k = V_i^2 g_k - V_i V_j (g_k cos\theta_k + b_k sin\theta_k) \tag{23}$$

$$Q_k = -V_i^2 b_k + V_i V_j (b_k cos\theta_k - g_k sin\theta_k) \tag{24}$$

$$V_i = V_{nom} + \Delta V_i,\ where\ \Delta V^{min} \le \Delta V_i \le \Delta V^{max} \tag{25}$$

Note that the voltage deviations at each node ΔV_i are expected to be very small. Substituting (25) in (23) and (24) and neglecting higher order terms, we get:

$$P_k \approx (V_{nom}^2 + 2V_{nom}\Delta V_i) g_k - (V_{nom}^2 + V_{nom}\Delta V_i + V_{nom}\Delta V_j)(g_k + b_k\theta_k) \tag{26}$$

$$Q_k \approx -(V_{nom}^2 + 2V_{nom}\Delta V_i) b_k + (V_{nom}^2 + V_{nom}\Delta V_i + V_{nom}\Delta V_j)(b_k - g_k\theta_k) \tag{27}$$

Note that equations (26) and (27) still contain nonlinearities because of the products of two continuous variables—voltage deviations and angle differences. However, since these variables ($\Delta V_i, \Delta V_j$ and θ_k) are very small, their products can be neglected. Hence, the above flow equations become:

$$P_k \approx V_{nom}(\Delta V_i - \Delta V_j) g_k - V_{nom}^2 b_k \theta_k \tag{28}$$

$$Q_k \approx -V_{nom}(\Delta V_i - \Delta V_j) b_k - V_{nom}^2 g_k \theta_k \tag{29}$$

The linear planning model proposed here is based on the above linearized flow equations. This linearization approach was first introduced in [45] in the context of transmission expansion planning problem.

When the investment planning includes switching and expansion of the distribution network system, equations (28) and (29) must be multiplied by the corresponding binary variables as in (30)-(33). This is to make sure the flow through an existing/a new feeder is zero when its switching/investment variable is zero; otherwise, the flow in that feeder should obey the Kirchhoff's Voltage Law.

$$P_k \approx u_{k,t}\{V_{nom}\left(\Delta V_i - \Delta V_j\right)g_k - V_{nom}^2 b_k \theta_k\} \tag{30}$$

$$Q_k \approx u_{k,t}\{-V_{nom}\left(\Delta V_i - \Delta V_j\right)b_k - V_{nom}^2 g_k \theta_k\} \tag{31}$$

$$P_k \approx x_{k,t}\{V_{nom}\left(\Delta V_i - \Delta V_j\right)g_k - V_{nom}^2 b_k \theta_k\} \tag{32}$$

$$Q_k \approx x_{k,t}\{-V_{nom}\left(\Delta V_i - \Delta V_j\right)b_k - V_{nom}^2 g_k \theta_k\} \tag{33}$$

The bilinear products, involving binary with voltage deviation and angle difference variables, introduces undesirable nonlinearity to the problem. This nonlinearity can be avoided using the big-M formulation i.e. by reformulating the above equations into their respective disjunctive equivalents as in (34)-(37). As a rule-of-thumb, the big-M parameter often set to the maximum transfer capacity in the system.

$$MP_k\left(u_{k,t} - 1\right) \leq P_{k,s,w,t} - \{V_{nom}\left(\Delta V_{i,s,w,t} - \Delta V_{j,s,w,t}\right)g_k - V_{nom}^2 b_k \theta_{k,s,w,t}\ )\} \leq MP_k\left(1 - u_{k,t}\right) \tag{34}$$

$$MQ_k\left(u_{k,t} - 1\right) \leq Q_{k,s,w,t} - \{-V_{nom}\left(\Delta V_{i,s,w,t} - \Delta V_{j,s,w,t}\right)b_k - V_{nom}^2 g_k \theta_{k,s,w,t}\} \leq MQ_k\left(1 - u_{k,t}\right) \tag{35}$$

$$MP_k\left(x_{k,t} - 1\right) \leq P_{k,s,w,t} - \{V_{nom}\left(\Delta V_{i,s,w,t} - \Delta V_{j,s,w,t}\right)g_k - V_{nom}^2 b_k \theta_{k,s,w,t}\} \leq MP_k\left(1 - x_{k,t}\right) \tag{36}$$

$$MQ_k\left(x_{k,t} - 1\right) \leq Q_{k,s,w,t} - \{-V_{nom}\left(\Delta V_{i,s,w,t} - \Delta V_{j,s,w,t}\right)b_k - V_{nom}^2 g_k \theta_{k,s,w,t}\} \leq MQ_k\left(1 - x_{k,t}\right) \tag{37}$$

3.3.2. Flow limits

The apparent power flow through a line $S_k$is given by $\sqrt{P_k^2 + Q_k^2}$ and this has to be less than or equal to the rated value which is denoted as:

$$P_k^2 + Q_k^2 \leq (S_k^{max})^2 \tag{38}$$

Considering line switching and investment, equation (38) can be rewritten as:

$$P_{k,s,w,t}^2 + Q_{k,s,w,t}^2 \leq u_{k,t}(S_k^{max})^2 \tag{39}$$

$$P_{k,s,w,t}^2 + Q_{k,s,w,t}^2 \leq x_{k,t}(S_k^{max})^2 \tag{40}$$

The quadratic expressions of active and reactive power flows in (39) through (40) can be easily linearized using piecewise linearization, considering a sufficiently large number of linear segments, L. There are a number of ways of linearizing such functions such as incremental, multiple choice, convex combination and other approaches in the literature [46]. Here, the first approach (which is based on first-order approximation of the nonlinear curve) is used because of its relatively simple formulation. To this end, two non-negative auxiliary variables are introduced for each of the flows P_k and Q_k such that $P_k = P_k^+ - P_k^-$ and $Q_k = Q_k^+ - Q_k^-$. Note that these auxiliary variables (i.e. P_k^+ , P_k^-, Q_k^+ and Q_k^-) represent the positive and negative flows of P_k and Q_k, respectively. This helps one to consider only the positive quadrant of the nonlinear curve, resulting in a significant reduction in the mathematical complexity, and by implication the computational burden. In this case, the associated linear constraints are:

$$P_{k,s,w,t}^2 \approx \sum_{l=1}^{L} \alpha_{k,l} p_{k,s,w,t,l} \tag{37}$$

$$Q_{k,s,w,t}^2 \approx \sum_{l=1}^{L} \beta_{k,l} q_{k,s,w,t,l} \tag{38}$$

$$P_{k,s,w,t}^+ + P_{k,s,w,t}^- = \sum_{l=1}^{L} p_{k,s,w,t,l} \tag{39}$$

$$Q_{k,s,w,t}^+ + Q_{k,s,w,t}^- = \sum_{l=1}^{L} q_{k,s,w,t,l} \tag{40}$$

where $p_{k,s,w,t,l} \leq \frac{P_k^{max}}{L}$ and $q_{k,s,w,t,l} \leq Q_k^{max}/L$.

3.3.3. Line losses

The active and reactive power losses in line k can be approximated as follows:

$$PL_k = P_{k,ij} + P_{k,ji} \approx 2V_{nom}^2 g_k (1 - cos\theta_k) \approx V_{nom}^2 g_k \theta_k^2 \tag{41}$$

$$QL_k = Q_{k,ij} + Q_{k,ji} \approx -2V_{nom}^2 b_k (1 - cos\theta_k) \approx -b_k V_{nom}^2 \theta_k^2 \tag{42}$$

Clearly, Equations (41) and (42) are nonlinear and nonconvex functions, making the problem more complex to solve. This can be overcome by having the quadratic angle differences piecewise-linearized, as it is done for the quadratic flows in the above. However, instead of doing this, the expressions in (41) and (42) can be expressed in terms of the active and the reactive power flows respectively by substituting θ_k from (7) and (8) in Equations (41) and (42) and neglecting higher order terms. This leads to (43) and (44).

$$PL_{k,s,w,t} = g_k \{P_{k,s,w,t}^2 - 2P_{k,s,w,t} V_{nom} (\Delta V_{i,s,w,t} - \Delta V_{j,s,w,t}) g_k\} / (V_{nom} b_k)^2 \tag{43}$$

$$QL_{k,s,w,t} = -b_k \{Q_{k,s,w,t}^2 + 2Q_{k,s,w,t} V_{nom} (\Delta V_{i,s,w,t} - \Delta V_{j,s,w,t}) b_k\} / (V_{nom} g_k)^2 \tag{44}$$

Note that expressing the losses as a function of flows has two advantages. First, doing so reduces the number of nonlinear terms that has to be linearized, which in turn results in a model with a reduced number of equations and variables. For example, if equations (41) and (42) are used instead, in addition to the quadratic power flow terms P_k^2 and Q_k^2, the quadratic angle differences θ_k^2 should also be linearized to make the problem linear and convex. On the contrary, if equations (43) and (44) are used, we are only required to linearize P_k^2 and Q_k^2. Second, it avoids unnecessary constraints on the angle differences when a line between two nodes is not connected or remains not selected for investment. In fact, this is often avoided by introducing binary variables and using a so-called big-M formulation [45]. However, this adds extra complexity to the problem.

Note that, in addition to the quadratic flow, equations (43) and (44) contain products of two continuous variables –flow and voltage magnitude deviations, which make the function non-separable. However, these products can be neglected because, in reality, the voltage deviation variables are expected to be very small, leading to the simplified equations (45) and (46) each having only the quadratic flow expressions.

$$PL_{k,s,w,t} = g_k P_{k,s,w,t}^2 / (V_{nom} b_k)^2 \tag{45}$$

$$QL_{k,s,w,t} = -b_k Q_{k,s,w,t}^2 / (V_{nom} g_k)^2 \tag{46}$$

3.3.4. Kirchhoff's current law (Active and reactive load balances)

Load balance should be respected all the time at each node i.e. the sum of all injections should be equal to the sum of all withdrawals at each node. This is enforced by adding the following two constraints:

$$\sum_{g\epsilon\Omega^{DG}}\left(P_{g,i,s,w,t}^E + P_{g,i,s,w,t}^N\right) + \sum_{es\epsilon\Omega^{es}}\left(P_{es,i,s,w,t}^{dch} - P_{es,i,s,w,t}^{ch}\right) + P_{\varsigma,s,w,t}^{SS} + \sum_{in,k\epsilon i} P_{k,s,w,t} - \sum_{out,k\epsilon i} P_{k,s,w,t} + \delta_{i,s,w,t} = D_{i,s,w,t} + PL_{\varsigma,s,w,t} + \sum_{k\epsilon i}\tfrac{1}{2}PL_{k,s,w,t} \; ; \; \forall\varsigma, \forall\varsigma\epsilon i \tag{47}$$

$$\sum_{g\epsilon\Omega^{DG}}(Q_{g,i,s,w,t}^E + Q_{g,i,s,w,t}^N) + \sum_{c\epsilon\Omega^c} Q_{c,i,s,w,t} + Q_{\varsigma,s,w,t}^{SS} + \sum_{in,k\epsilon i} Q_{k,s,w,t} - \sum_{out,k\epsilon i} Q_{k,s,w,t} = Q_{i,s,w,t} + QL_{\varsigma,s,w,t} + \sum_{in,k\epsilon i}\tfrac{1}{2}QL_{k,s,w,t} + \sum_{out,k\epsilon i}\tfrac{1}{2}QL_{k,s,w,t} \; ; \; \forall\varsigma, \forall\varsigma\epsilon i \tag{48}$$

Equations (47) and (48) stand for the active and the reactive power balances at each node, respectively.

3.3.5. Bulk Energy Storage Model Constraints

The generic bulk Energy Storage (ES) is modeled by equations (49)-(57).

$$0 \le P_{es,i,s,w,t}^{ch} \le I_{es,i,s,w,t}^{ch} x_{es,i,t} P_{es,i}^{ch,max} \tag{49}$$

$$0 \le P_{es,i,s,w,t}^{dch} \le I_{es,i,s,w,t}^{dch} x_{es,i,t} P_{es,i}^{dch,max} \tag{50}$$

$$I_{es,i,s,w,t}^{ch} + I_{es,i,s,w,t}^{dch} \le 1 \tag{51}$$

$$E_{es,i,s,w,t} = E_{es,i,s,w-1,t} + \eta_{ch,es} P_{es,i,s,w,t}^{ch} - \eta_{dch,es} P_{es,i,s,w,t}^{dch} \tag{52}$$

$$E_{es,i}^{min} x_{es,i,t} \le E_{es,i,s,w,t} \le x_{es,i,t} E_{es,i}^{max} \tag{53}$$

$$E_{es,i,s,w_0,T1} = \mu_{es} x_{es,i,T1} E_{es,i}^{max} \tag{54}$$

$$E_{es,i,s,w_1,t+1} = E_{es,i,s,W,t} \tag{55}$$

The limits on the capacity of ES while being charged and discharged are considered in equations (49) and (50), respectively. Inequality (51) prevents simultaneous charging and discharging operation of ES at the same operational time w. The amount of stored energy within the reservoir of bulk ES at the operational time w as a function of energy stored until $w-1$ is given by (52). The maximum and minimum levels of storages in operational time w are also considered through inequality (53). Equations (54) shows the initial level of stored energy in the bulk ES as a function of its maximum reservoir capacity. In a multi-stage planning approach, Equation (55) ensures that the initial level of energy in the bulk ES at a given year is equal to the final level of energy in the ES in the preceding year. Here, $\eta_{dch,es}$is assumed to be $1/\eta_{ch,es}$.

Notice that inequalities (49) and (50) involve products of charging/discharging binary variables and investment variable. In order to linearize this, new continuous positive variables $z_{es,i,s,w,t}^{ch}$, and $z_{es,i,s,w,t}^{dch}$, which replaces the bilinear products in each constraint, is introduced such that the set of linear constraints in (56) and (57) hold. For instance, the product $I_{es,i,s,w,t}^{dch} x_{es,i,t}$ is replaced by the positive variable $z_{es,i,s,w,t}^{dch}$. Then, the bilinear product is decoupled by introducing the set of constraints in (56) [47].

$$z_{es,i,s,w,t}^{dch} \leq x_{es}^{max} I_{es,i,s,w,t}^{dch} \text{ ; } z_{es,i,s,w,t}^{dch} \leq x_{es,i,t} \text{ ; } z_{es,i,s,w,t}^{dch} \geq x_{es,i,t} - \left(1 - I_{es,i,s,w,t}^{dch}\right) x_{es}^{max} \quad (56)$$

Similarly, the product $I_{es,i,s,w,t}^{ch} x_{es,i,t}$is decoupled by including the following set of constraints:

$$z_{es,i,s,w,t}^{ch} \leq x_{es}^{max} I_{es,i,s,w,t}^{ch} \text{ ; } z_{es,i,s,w,t}^{ch} \leq x_{es,i,t} \text{ ; } z_{es,i,s,w,t}^{ch} \geq x_{es,i,t} - \left(1 - I_{es,i,s,w,t}^{ch}\right) x_{es}^{max} \quad (57)$$

3.3.6. Active and reactive power limits of DGs

The active and reactive capacity limits of existing generators are given by (58) and (59), respectively. In the case of candidate generators, the corresponding constraints are (60) and (61). Note that the binary variables also appear here and multiply the minimum and the maximum generation capacities of a given generator. This is to make sure that the power generation variable is zero when the generator remains either unutilized or unselected for investment.

$$P_{g,i}^{E,min} u_{g,i,t} \leq P_{g,i,s,w,t}^{E} \leq P_{g,i}^{E,max} u_{g,i,t} \quad (58)$$

$$Q_{g,i}^{E,min} u_{g,i,t} \leq Q_{g,i,s,w,t}^{E} \leq Q_{g,i}^{E,max} u_{g,i,t} \quad (59)$$

$$P_{g,i}^{N,min} x_{g,i,t} \leq P_{g,i,s,w,t}^{N} \leq P_{g,i}^{N,max} x_{g,i,t} \quad (60)$$

$$Q_{g,i}^{N,min} x_{g,i,t} \leq Q_{g,i,s,w,t}^{N} \leq Q_{g,i}^{N,max} x_{g,i,t} \quad (61)$$

3.3.7. Reactive power limit of capacitor banks

Inequality (62) ensures that the reactive power produced by the capacitor banks is bounded between zero and the maximum capacity.

$$0 \leq Q_{c,i,s,w,t} \leq x_{c,i,t} Q_c^0 \quad (62)$$

3.3.8. Active and reactive power limits of power purchased

For technical reasons, the power that can be purchased from the transmission grid could have minimum and maximum limits, which is enforced by (63) and (64). However, it is understood that setting the maximum and minimum limits is difficult. These constraints are included here for the sake of completeness. In this work, these limits are set to 1.5 times the minimum and maximum levels of total load in the system. Note that the multiplier is higher than one because the system has losses, which needs to be covered by generating extra power.

$$P^{SS,min}_{\varsigma,s,w,t} \leq P^{SS}_{\varsigma,s,w,t} \leq P^{SS,max}_{\varsigma,s,w,t} \tag{63}$$

$$Q^{SS,min}_{\varsigma,s,w,t} \leq Q^{SS}_{\varsigma,s,w,t} \leq Q^{SS,max}_{\varsigma,s,w,t} \tag{64}$$

3.3.9. Logical constraints

The following logical constraints ensure that an investment decision cannot be reversed i.e. an investment already made cannot be divested.

$$x_{k,t} \geq x_{k,t-1} \tag{65}$$

$$x_{g,i,t} \geq x_{g,i,t-1} \tag{66}$$

$$x_{es,i,t} \geq x_{es,i,t-1} \tag{67}$$

$$x_{c,i,t} \geq x_{c,i,t-1} \tag{68}$$

3.3.10. Radiality constraints

There are two conditions that must be fulfilled in order a distribution network system (DNS) to be radial. First, the solution must have $N_i - N_{SS}$ circuits. Second, the final topology should be connected. Equation (69) represents the first necessary condition for maintaining the radial topology of DNs.

$$\sum_{k\in\Omega^{ij}} OR(x_{k,t}, u_{k,t}) = N_i - N_{SS} \quad ;\forall t \tag{69}$$

Note that the above equation assumes line investment is possible in all corridors. Hence, in a given corridor, we can have either an existing branch or a new one, or both connected in parallel, depending on the economic benefits of the final setup (solution) brings about to the system. The radiality constraint in (69) then has to accommodate this condition. One way to do this is using the Boolean logic operation, as in (69). Unfortunately, this introduces nonlinearity. We show how this logic can be linearized using an additional auxiliary variable $z_{k,t}$ and the binary variables associated to existing and new branches i.e. $u_{k,t}$ and $x_{k,t}$, respectively. Given $z_{k,t} := OR(x_{k,t}\ ,\ u_{k,t})$, this Boolean operation can be expressed using the following set of linear constraints:

$$z_{k,t} \leq x_{k,t} + u_{k,t};\ z_{k,t} \geq x_{k,t};\ z_{k,t} \geq u_{k,t}; 0 \leq z_{k,t} \leq 1 \quad ;\forall t \tag{70}$$

Note that the auxiliary variable $z_{k,t}$ is automatically constrained to be binary. Hence, it is not necessary to explicitly define $z_{k,t}$ as a binary variable; instead, defining it as a continuous positive variable is sufficient. Alternatively, if $z_{k,t}$ is defined to be binary variable from the outset, then, equation (69) can be converted into a single range constraint as:

$$0 \leq 2z_{k,t} - x_{k,t} - u_{k,t} \leq 1 \quad ; \forall t \tag{71}$$

Then, the radiality constraints in (69) can be reformulated using the $z_{k,t}$ variables as:

$$\sum_{k \in \Omega^{ij}} z_{k,t} = N_i - N_{SS} \quad ; \forall t \tag{72}$$

When all loads in the DNS are only fed by power from substations, the final solution obtained automatically satisfies the two aforementioned conditions; hence, no additional constraints are required i.e. (70) or (71) along with (72) are sufficient to guarantee radiality. However, it should be noted that in the presence of DGs and reactive power sources, these constraints alone may not ensure the radiality of the distribution network, as pointed out in [48] and further discussed in [49]. This is however out of the scope of this work. If this is indeed found out to be a critical issue, additional constraints need to be added to guarantee that all buses are linked, as proposed in [43], [49–51].

5. Uncertainty and Variability Management

There are various sources of uncertainty and variability in a distribution systems planning problem, particularly with intermittent renewable sources. These are related to the variability in time and the randomness of operational situations [52]. In addition, there are other uncertainties mostly related to the long-term electricity, carbon and fuel prices, rules, regulations and policies, etc. Exhaustive modeling of all sources of uncertainty and variability is out of the scope of this work. However, variabilities due to intermittent DG power outputs (mainly, wind and solar) and demand are captured by considering a sufficiently large number of operational states, also known as here “snapshots”. To ensure tractability, a standard clustering technique (*k-means*) is used to reduce the number of snapshots to 200. Here, each cluster represents a group of similar operational situations. A representative snapshot, the medoid in this case, is then selected from each cluster. And, a weight is assigned to each representative snapshot, which is proportional to the number of operational situations in its group.

The hourly demand at each node (which is largely predictable) is assumed to be available. Here, an hourly demand series of a real-life distribution network is considered. Wind speed is assumed to follow a Weibull probability distribution. A total of 8760 samples (corresponding to the number of hours in a year) are generated randomly from this probability distribution. Similarly, the hourly solar radiation is assumed to follow beta probability distribution, and the same number of samples is generated accordingly. Note that these generated random samples cannot be used as they are in the planning process. They should be readjusted to reflect the temporal correlations that naturally exist among demand, solar radiation and wind speed series. To this end, the correlation between wind and solar sources is considered to be -0.3 while that of wind and demand is 0.28, which is in line with the results in [53]. A correlation of 0.5 is assumed between solar and demand, according to [54]. Using these correlations and the demand series as a reference, the wind speed and solar radiation time series are readjusted by making use of Cholesky Factorization, which can easily be implemented in MATLAB™. This way, new wind speed and solar radiation series are obtained that meet the mentioned inter-correlations. Then, the hourly wind and solar power output are determined by plugging in these readjusted series into their corresponding power curves given by equations (73) and (74).

$$P_{wnd,h} = \begin{cases} 0 & ; 0 \leq v_h \leq v_{ci} \\ P_r\left(A + Bv_h^3\right) & ; v_{ci} \leq v_h \leq v_r \\ P_r & ; v_r \leq v_h \leq v_{co} \\ 0 & ; v_h \leq v_{co} \end{cases} \tag{73}$$

In the above equation, A and B are parameters represented by the expressions in [55] and [56]. Similarly, the hourly solar power output $P_{sol,h}$ is determined by plugging in the hourly solar radiation levels in the solar power output expression given in **Erro! A origem da referência não foi encontrada.**, [57].

$$P_{sol,h} = \begin{cases} \frac{P_r R_h^2}{R_{std} * R_c} & ; 0 \leq R_h \leq R_c \\ \frac{P_r R_h}{R_{std}} & ; R_c \leq R_h \leq R_{std} \\ P_r & ; R_h \geq R_{std} \end{cases} \tag{74}$$

6. Case Study

6.1. System data and assumptions

The distribution network system, shown in Figure 1, is used to test the developed planning model. Information regarding network and maximum demand data is provided in Table A. 1 (Appendix A,) [58]. The total active and reactive loads in the system are 4.635 MW and 3.25 MVAr, respectively. The nominal voltage of the system is 12.66 kV. The following assumptions are made when carrying out the simulation:

- A 3-year planning horizon is considered, which is divided into yearly decision stages.
- Interest rate is set to 7%.
- For the sake of simplicity, maintenance costs are taken to be 2% of the corresponding investment costs.
- The lifetime of capacitor banks and energy storage systems is assumed to be 15 years, while that of DGs and feeders is 25.
- A 5% voltage deviation is considered to be the maximum allowable deviation in the system.
- The power transfer capacity of all feeders is assumed to be 6.986 MVA.
- All big-M parameters are set to 10, which is higher than the power transfer capacity of all feeders.
- The number of piecewise linear segments is limited to 5. This balances well accuracy with computation burden, as concluded in [59].
- The efficiency of the bulk ES is assumed to be 90%.
- The unit cost of capacitor banks is assumed to be €25/kVAr.
- The size of the minimum deployable capacitor bank is considered to be 0.1 MVAr.

- The investment cost of a 1.0 MW bulk ES, whose energy reservoir is 5 MWh, is considered to be 1.0 M€.
- The emission rate of power purchased is arbitrarily set to 0.4 tCO_2e/MWh.
- The investment cost of a given feeder is assumed to be directly proportional to its impedance i.e. $C_{ij} = constant * Z_{ij}$ where the proportionality constant is 10,000 €/Ω.
- Wind and solar type DGs, each with 1 MW installed capacity, are considered as potential candidates to be deployed in the system. The investment costs of these generators is assumed to be 2.64 M€ and 3 M€, respectively.
- Yearly demand growths of 5%, 10% and 15% are assumed for the planning stages.
- The emission prices in the first, second and third stages are set to 25, 45 and 60 €/ tCO_2e, respectively.
- Variable power generation sources (wind and solar, in particular) are assumed to be available in every node. This assumption emanates from the fact that distribution networks span over a small geographical area. Hence, the distribution of resources in this area can be considered to be the same.
- The substation node (node 1) is considered as a reference; hence, its voltage magnitude and angle are set to $1.02 * V_{nom}$and 0, respectively.
- The cost of unserved energy is set to 3000 €/MWh.

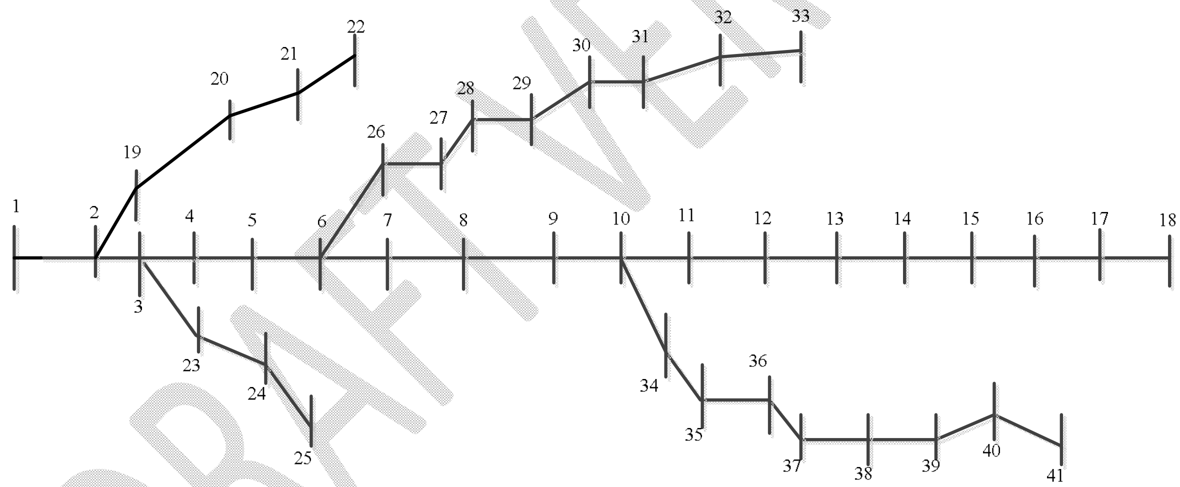

Figure 1. Single-line diagram of the IEEE 41-bus distribution network system.

6.2. Results and Discussion

Intermittent power generation sources such as wind and solar PV type DGs normally operate with a fixed leading power factor [60]. In other words, such generators absorb reactive power, instead of producing and contributing to the voltage regulation in the system (also known as reactive power support). In power systems, voltage regulation has been traditionally supported by conventional (synchronous) generators. However, this is likely to change in the near future given the upward trend of integrating such resources in power systems. These generators will be equipped with reactive power support devices, which are predominantly based on power electronics, to enhance their capability to provide reactive power when it is needed in the system. Here, we have carried out the system expansion considering without reactive power support, and the results of the simulation are discussed as follows.

The power factor of wind and solar PV type DGs is set to 0.95 leading [60]. This means such DGs consume reactive power all the time. The system is expanded considering this case, and the expansion results are discussed below.

The optimal solution for capacitor banks, DGs and bulk ES in the system are shown in Tables 1 through 3, respectively. In general, majority of the investments are made in the first stage. This is because the NPV of operation and emission costs are higher in the first stage than those in any of the subsequent stages. This makes it attractive to invest more in renewables in the first stage than in the other stages so that these costs are drastically reduced.

As we can see in Table 1, the optimal location of capacitor banks mostly coincide with high load connection points (nodes) as well as with those closer to the end nodes. This is expected from the system operation point of view because capacitor banks are required at such nodes to meet the reactive power requirements and thus keep the corresponding voltages within allowable operational limits. Otherwise, the voltages are expected to drop at these nodes without a compensation mechanism put in place. As shown in Figure 2, the total size of investment in capacitor banks required throughout the planning horizon is 4.0 MVAr, out of which investments in 3.4, 0.1 and 0.5 MVAr are made in the first, second and third stages, respectively.

Table 2 shows that more investments are made in wind than in solar PV type DGs. This is because of the higher capacity factor of potential wind power generators compared to solar PV ones. In general, the total MW of DG power installed at each node and stage in the system is shown in Figure 2. Here, the optimal size of DGs integrated in the system is 8 and 2 MW in the first and the third stages, respectively.

Table 1. Optimal investment solution for capacitor banks at each stage

Location (Bus)	Time stages T1	T2	T3
		$x_{c,i,t}$	
7	1	1	1
8	4	4	4
14	4	4	4
24	0	0	2
25	1	1	3
29	1	1	1
30	8	9	9
31	1	1	1
32	2	2	2
37	1	1	1
38	8	8	9
39	1	1	1
40	2	2	2

Table 2. Optimal investment solution for DGs at each stage

DG type	Location (Bus)	Time stages T1	T2	T3
			$x_{g,i,t}$	
Solar	30	1	1	1
Wind	7	0	0	1
Wind	14	2	2	2
Wind	18	1	1	1
Wind	30	1	1	1
Wind	31	1	1	1
Wind	37	1	1	2
Wind	38	1	1	1

Table 3. Optimal investment solution for bulk energy storage at each stage

Location (Bus)	Time stages T1	T2	T3
		$x_{es,i,t}$	
14	2	2	2
30	1	1	1
39	2	2	2

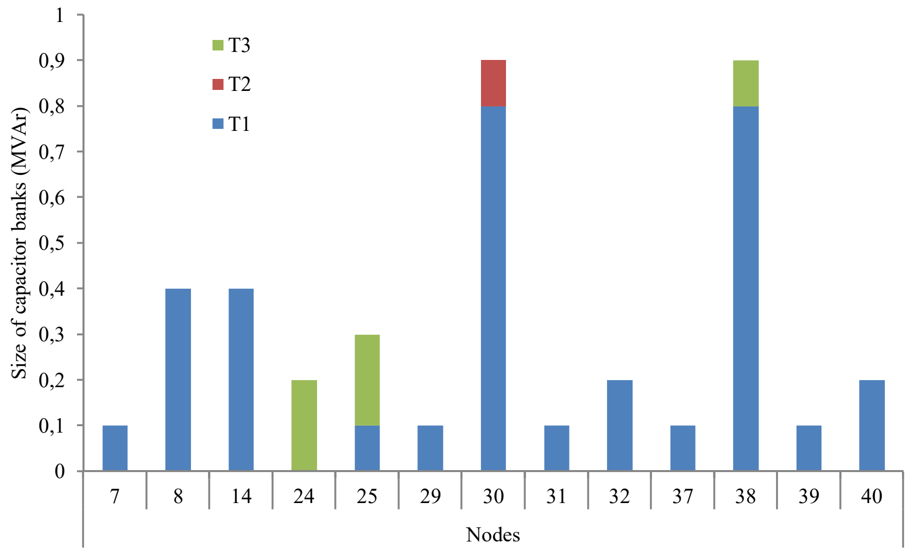

Figure 2. Optimal location and size of capacitor banks at each stage

The results in Tables 1 through 3 (also conveniently shown in Figure 3) demonstrate the strong complementarity of variable generation, energy storage systems and compensators. Based on the results here, the bulk ES systems and DGs in particular are optimally located close to one another.

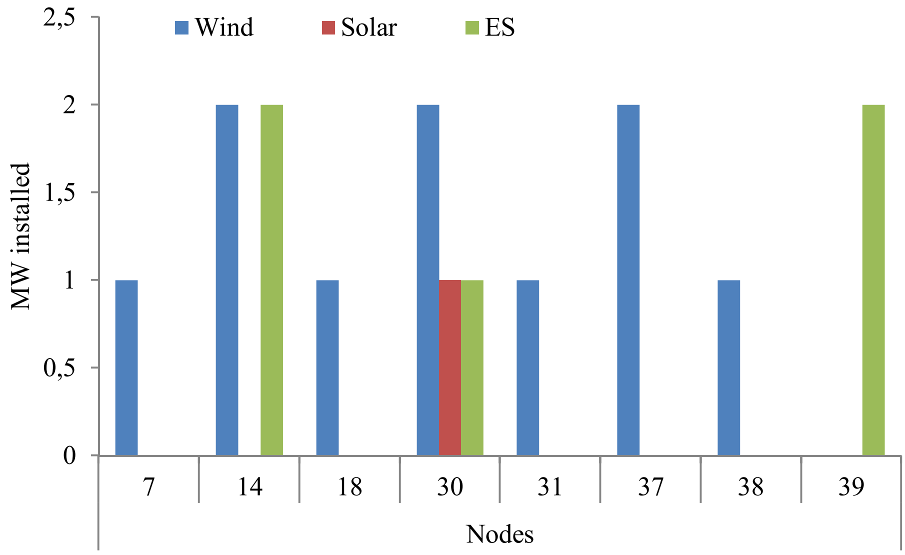

Figure 3. Optimal size of energy storage, installed solar and wind power at each node throughout the planning horizon.

It is well known that bulk ES can bring significant benefits such as load following, power stability improvements, and enhancing the dispatchability of RESs from the system operator's point of view according to their operation modes. Likewise, the optimal deployment of capacitor banks also brings substantial benefits to system. The combination of all these entirely helps one to dramatically increase the size of RESs that can be integrated into the system without violating system constraints. The optimal size of RESs would, otherwise, be limited to only 3 MW. It is interesting to see here that the integration of ESs and capacitor banks has such a dramatic impact on the level of DG integration. This is due to the fact that ESSs and capacitor banks bring about significant flexibility and control mechanism to the system. Substantial improvements in voltage controllability are also clearly visible in Figures 4 and 5. These figures show the voltage deviation profiles at each node with the selected operational situations (which can alternatively be understood as "long hours") without and with system expansion, respectively. In the base case (shown in Figure 4), one can see that some of the node voltage deviations (especially those at the extreme nodes) tend to be very close to the minimum allowable limit. On the contrary, all node voltages largely stay very close to the nominal one (with an average deviation of approximately 1.5%), leaving significant margins to the operational limits. Alternatively, Figure 6 conveniently shows the variance of the voltage deviations at each node. It is also evident to see here that the variance of most of the deviations is very low. The highest variances at nodes 20 to 22 are due to high impedance of feeder connected between nodes 19 and 20 (see Table A. 1 in Appendix A). The same reasoning explains the relatively high variances in nodal voltage deviations between nodes 13 and 18. However, these variances are negligible when put in perspective with the square of maximum deviation, i.e. $(\Delta V^{max})^2$, which in this case is approximately $(0.05 * 12.66kV)^2 \approx 400000\, V^2$. In general, such a substantial improvement in voltage controllability has come from the combined effect of expansion decisions in DG, ES and capacitor banks.

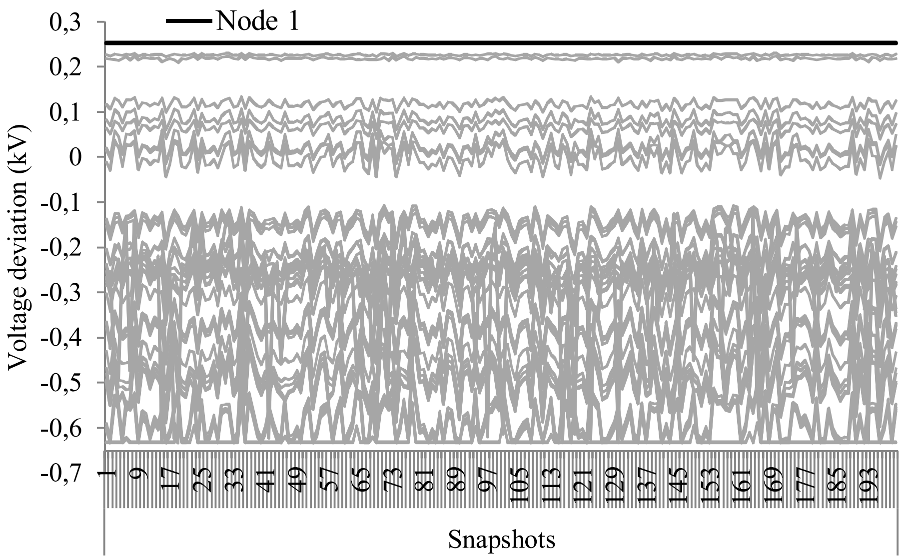

Figure 4. Profiles of voltage deviations without system expansion in the first stage.

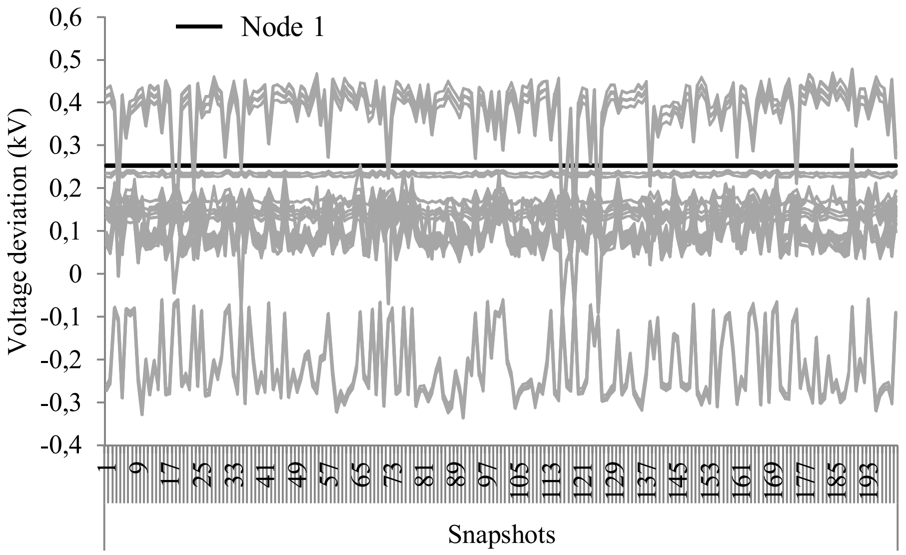

Figure 5. Profiles of voltage deviations at each node after expansion in the first stage

Other important aspects in this expansion analysis are related to the impact of system expansion on the network losses and investments. Figure 7 shows a comparison of the network losses in the base case and with expansion for every operational state. We can see a significant reduction in network losses (by nearly 50% on average) in the system after the expansion planning is carried out. This is one of the major benefits of integrating DGs in the system. Concerning investments in lines, in this particular case study, not a single feeder is selected for reinforcements. This clearly indicates line investments are deferred when DGs are integrated in the system.

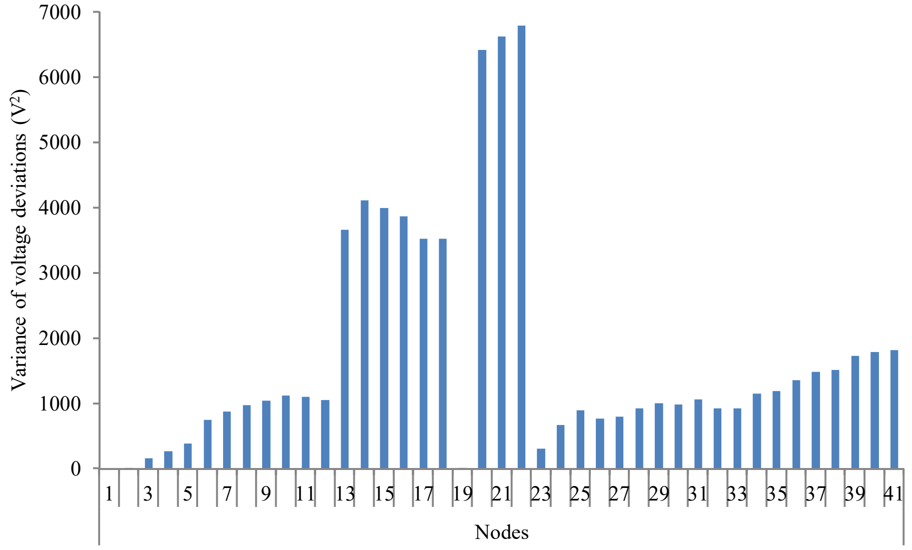

Figure 6. Variance of voltage deviations at each node as a result of variations in system operational states

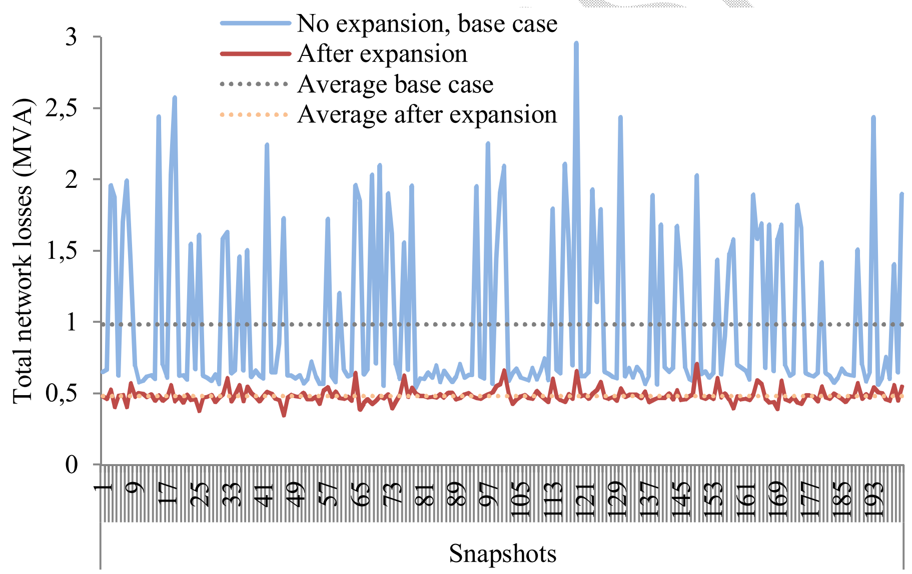

Figure 7. Network losses with and without system expansion (first stage).

For this particular case study, the total NPV investment costs for the three stages are 30.427, 0.003 and 5.294 M€, respectively, bringing the total investment costs to 37.724 M€. And, the NPV cost of energy, emissions, maintenance and unserved power throughout the planning horizon for the corresponding stages are 27.105, 8.089, 9.442 and 0.868 M€, respectively. The overall NPV cost in this case is 83.228 M€.

6.3. A strategy for reducing combinatorial search space

In the case study presented above, all nodes in the system are assumed to be candidates for the placement of DGs, ESS and capacitor banks. However, this is not possible when the planning work is carried out on large-scale DNSs because the size of the problem becomes huge as a result of combinatorial explosion, rendering difficulty in solving the problem to optimality. Owing to this fact, the potential candidate nodes are often predetermined either arbitrarily or using some criteria for the selection such as the level of load, availability of resources, etc. For example, the possible connection points of RES-based DGs are often known a priori based on the availability of primary energy sources (such as wind speed and solar radiation). In fact, the variation in the availability of wind speed and solar radiation among the connection points in the DNS is not expected to be significant because it normally spans over a geographically small area.

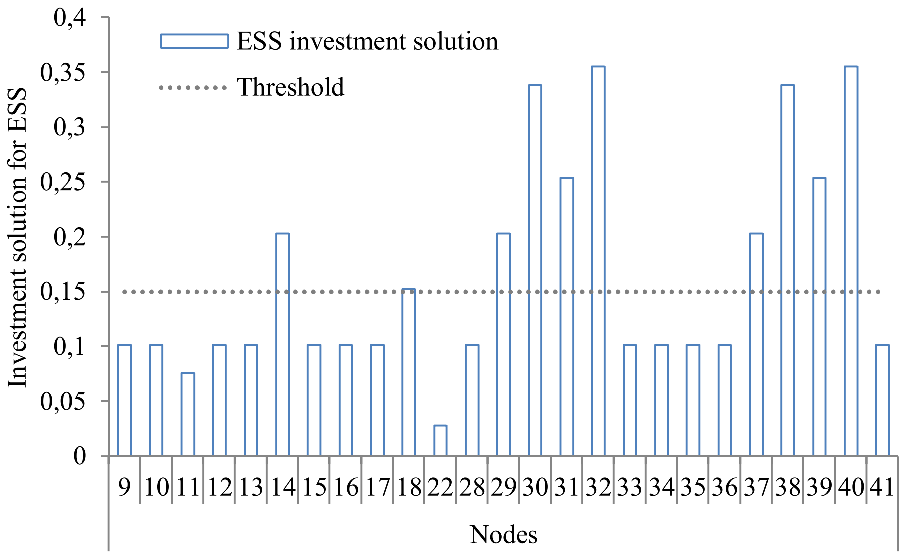

Figure 8. Decision variable for ESS at each node (last stage).

Here, we show how the combinatorial search space can be substantially reduced using a simple heuristic method. The method is based on solving a relaxed version of the original problem. This is done by treating all (normally integer) investment variables except the line reinforcement variables as continuous ones. This effectively means fractional investment decisions are allowed. The method here works by first establishing a threshold for each fractional investment solution (i.e. corresponding to DGs, ESS and capacitor banks). Then, those nodes whose corresponding values of investment solutions are lower than the preset thresholds are neglected. For instance, consider the investment solution of the relaxed problem corresponding to ESS at each node, as shown in Figure 8. In this case, the threshold is set to 0.15. As we can see, for most of the nodes, the investment values corresponding to ESS fall below this threshold. Only those values at the following nodes are significant: $\{14, 18, 29, 30, 31, 32, 37, 38, 39, 40\}$. This set of nodes is hence considered as the most likely locations in the system for ESS placements in the “brute force” planning model (i.e. the full MILP version). It should be noted that such a reduction in possible connection points (from 41 to 10) results in a substantial reduction of the combinatorial search space, by implication the computational burden. Note that the procedure/criterion for setting the threshold is an open question.

Similarly, the reduced set of nodes for possible capacitor and DG connections are obtained by using 1 and 0.2 as thresholds, respectively, as shown in Figure 9 and 10. In this case,

$\{7, 8, 14, 24, 25, 29, 30, 31, 32, 37, 38, 39, 40\}$ is the reduced set of nodes for capacitor bank connections, and that of DGs is $\{7, 8, 14, 18, 25, 29, 30, 31, 32, 37, 38, 39, 40\}$.

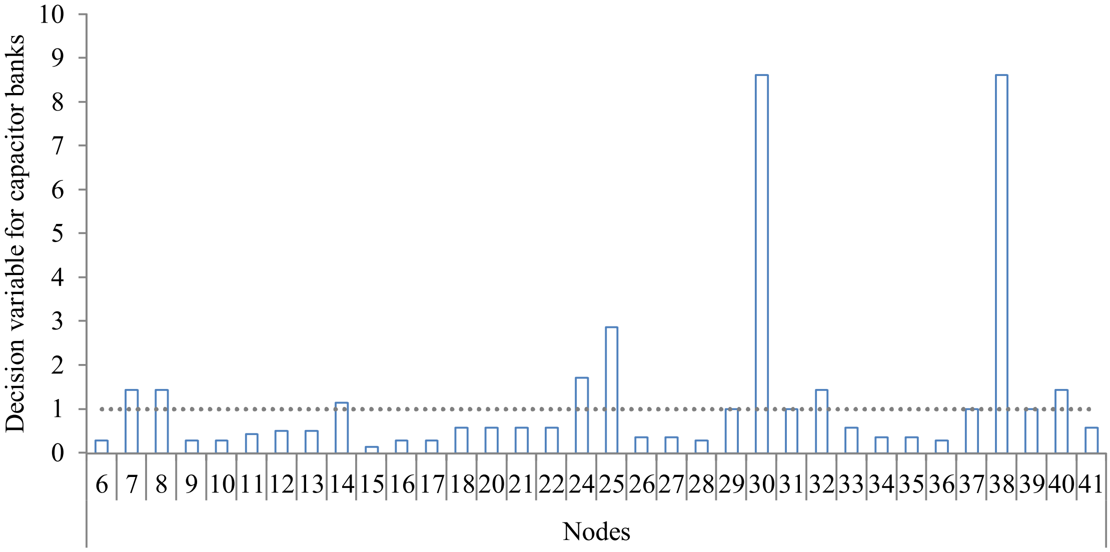

Figure 9. Investment solution for capacitor banks at each node (last stage).

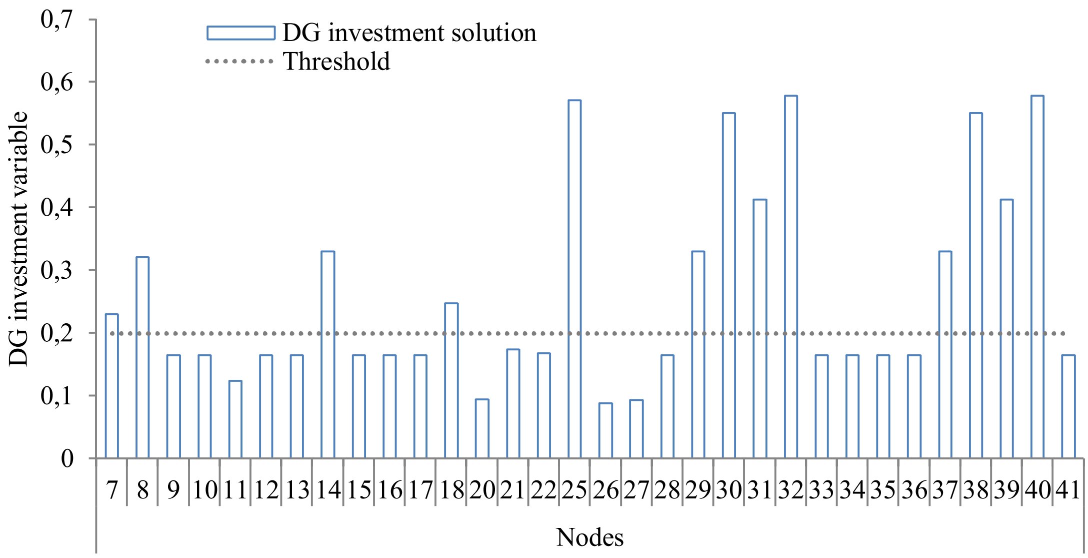

Figure 10. Investment solution for DGs at each node (last stage).

The heuristic method, proposed here, has been applied in the case study, and the results are compared with that of the "brute force" model. The investment decisions remain the same in both cases but the computational requirements substantially differ from one another. This heuristic method has significantly reduced the combinatorial solution search space and thus the computational effort by more than sevenfold.

7. Conclusions

This work has developed a new joint multi-stage mathematical optimization model considering smart-grid enabling technologies such as ESS, compensators, and network switching and/or expansion to support large-scale DG integration. The integrated planning model simultaneously determines the optimal sizing, time and placement of ESSs and compensators as well as that of RESs in distribution networks. The ultimate goal of this optimization work is to maximize the RES power absorbed by the system while maintaining the power quality and stability at the required/standard levels at a minimum cost possible. The model, formulated as a MILP optimization, employs a linearized AC network model which better captures the inherent characteristics of power network systems and balances accuracy with computational burden. The standard IEEE 41-bus distribution system is used to test the developed model and carry out the required analysis from the standpoint of the objectives set in this work.

The results of the case study show that the integration of energy storage systems and compensators helps to significantly increase the size of variable generation (wind and solar) in the system. For the case study, a total of 10 MW demand wind and solar power has been added to the system One can put this into perspective with the peak load 4.635 MW in the system. This means it has been possible to integrate RES power more than twice the peak demand in the base case. It has been demonstrated that the joint planning of DGs, compensators and ES systems, proposed in this work, brings about significant improvements to the system such as reduction of losses, cost of electricity and emissions, voltage support and many more others.

The expansion planning model proposed here can be considered as a major leap forward towards developing controllable grids, which support large-scale integration of RESs (as opposed to the conventional "fit and forget" approach). It can also be a handy tool to speed up the integration of more RESs until smart grids are realized in the future.

APPENDIX A. INPUT DATA

Table A. 1 Load and network data for the IEEE 41-bus distribution network system

	Demand data		Network data					
Node	Active power (kW)	Reactive power (kVAr)	From node	To node	Resistance (Ω)	Reactance (Ω)	Capacity (MVA)	Investment cost (x 1000 €)
2	100	60	1	2	0.0992	0.0470	6.9860	0.9920
3	90	40	2	3	0.4930	0.2511	6.9860	4.9300
4	120	80	3	4	0.3660	0.1864	6.9860	3.6600
5	60	30	4	5	0.3811	0.1941	6.9860	3.8110
6	60	20	5	6	0.8190	0.7070	6.9860	8.1900
7	200	100	6	7	0.1872	0.6188	6.9860	1.8720
8	200	100	7	8	0.7114	0.2351	6.9860	7.1140
9	60	20	8	9	10.300	0.7400	6.9860	103.00
10	60	20	9	10	10.440	0.7400	6.9860	104.40
11	45	30	10	11	0.1966	0.0650	6.9860	1.9660
12	60	35	11	12	0.3744	0.1238	6.9860	3.7440
13	60	35	12	13	14.680	11.550	6.9860	146.80

14	120	80	13	14	0.5416	0.7129	6.9860	5.4160
15	60	10	14	15	0.5910	0.5260	6.9860	5.9100
16	60	20	15	16	0.7463	0.5450	6.9860	7.4630
17	60	20	16	17	12.890	17.210	6.9860	128.90
18	90	40	17	18	0.7320	0.5470	6.9860	7.3200
19	90	40	2	19	0.1640	0.1565	6.9860	1.6400
20	90	40	19	20	15.042	13.554	6.9860	150.42
21	90	40	20	21	0.4095	0.4784	6.9860	4.0950
22	90	40	21	22	0.7089	0.9373	6.9860	7.0890
23	90	50	3	23	0.4512	0.3083	6.9860	4.5120
24	420	200	23	24	0.8980	0.7091	6.9860	8.9800
25	420	200	24	25	0.8960	0.7011	6.9860	8.9600
26	60	25	6	26	0.2030	0.1034	6.9860	2.0300
27	60	25	26	27	0.2842	0.1447	6.9860	2.8420
28	60	20	27	28	10.590	0.9337	6.9860	105.90
29	120	70	28	29	0.8042	0.7006	6.9860	8.0420
30	200	600	29	30	0.5075	0.2585	6.9860	5.0750
31	150	70	30	31	0.9744	0.9630	6.9860	9.7440
32	210	100	31	32	0.3105	0.3619	6.9860	3.1050
33	60	40	32	33	0.3410	0.5302	6.9860	3.4100
34	60	25	10	34	0.2030	0.1034	6.9860	2.0300
35	60	25	34	35	0.2842	0.1447	6.9860	2.8420
36	60	20	35	36	10.590	0.9337	6.9860	105.90
37	120	70	36	37	0.8042	0.7006	6.9860	8.0420
38	200	600	37	38	0.5075	0.2585	6.9860	5.0750
39	150	70	38	39	0.9744	0.9630	6.9860	9.7440
40	210	100	39	40	0.3105	0.3619	6.9860	3.1050
41	60	40	40	41	0.3410	0.5302	6.9860	3.4100

NOMENCLATURE

a) Sets/Indices

t/Ω^t	Index/set of time stages
$g/\Omega^g/\,\Omega^{DG}$	Index/set of DGs
i/Ω^i	Index/set of buses
es/Ω^{es}	Index/set of energy storages
c/Ω^c	Index/set of capacitor banks
s/Ω^s	Index/set of scenarios
w/Ω^w	Index/set of snapshots
$ç/\Omega^ç$	Index/set of substations
k/Ω^ℓ	Index/set of branches
h	Index for hours

b) Parameters

r	Interest rate

$IC_{g,i}, IC_k, IC_{es,i}, IC_{c,i}$	Investment cost of DG, line, energy storage system and capacitor banks, respectively
$LT_g, LT_k, LT_{es,} LT_c$	Lifetimes of DG, line, energy storage system and capacitor banks, respectively
MC_g^N, MC_g^E	Maintenance costs of new and existing DGs per year
MC_k^N, MC_k^E	Maintenance costs of new and existing branch *k* per year
MC_c, MC_{es}	Maintenance cost of capacitor bank and energy storage system per year
ρ_s, π_w	Probability of scenario *s* and weight (in hours) of snapshot group *w*
$OC_{g,i,s,w,t}^N, OC_{g,i,s,w,t}^E$	Cost of unit energy production by new and existing DGs
$\gamma_{es,i,s,w,t}^{dch}$	Cost of energy discharged from storage system
$\sigma_{\varsigma,s,w,t}$	Price of electricity purchased from upstream
$\upsilon_{s,w,t}$	Penalty for unserved power
$\lambda_{s,w,t}^{CO_2e}$	Price of emissions (€/tons of CO_2 equivalent—€/tCO_2e)
$ER_g^N, ER_g^E, ER_\varsigma^{SS}$	Emission rates of new and existing DGs, and energy purchased at sub-stations, respectively
g_k, b_k, S_k^{max}	Conductance, susceptance and flow limit of branch *k*
MP_k, MQ_k	Big-M parameters associated to active and reactive power flows through link *k*, respectively
α_l, β_l	Slopes of linear segments
L	Total number of linear segments
$P_{es,i}^{ch,max}, P_{es,i}^{dch,max}$	Charging and discharging power limits of a storage system
$\eta_{ch,es}, \eta_{dch,es}$	Charging and discharging efficiencies of a storage system
$E_{es,i}^{min}, E_{es,i}^{max}$	Energy storage limits
Q_c^0	Rating of minimum capacitor bank
N_i, N_{SS}	Number of buses and substations, respectively
$P_{wnd,h}$	Hourly wind power output
$P_{sol,h}$	Hourly solar PV output
P_r	Rated power a DG unit
v_h	Observed/sampled hourly wind speed
v_{ci}	Cut-in wind speed
v_r	Rated wind speed
v_{co}	Cut-out wind speed
R_c	A certain radiation point (often taken to be 150 W/m^2)
R_{std}	Solar radiation in standard condition (usually set to 1000 W/m^2)
R_h	Hourly solar radiation

c) Variables

$x_{g,i,t}, x_{es,i,t}, x_{c,i,t}, x_{k,t}$	Investment variables for DG, energy storage system, capacitor banks and distribution lines
$u_{g,i,t}, u_{k,t}$	Utilization variables of existing DG and lines
$P_{g,i,s,w,t}^N, P_{g,i,s,w,t}^E$	Active power produced by new and existing DGs
$Q_{g,i,s,w,t}^N, Q_{g,i,s,w,t}^E$	Reactive power produced by new and existing DGs
$P_{\varsigma,s,w,t}^{SS}, Q_{\varsigma,s,w,t}^{SS}$	Active and reactive power imported from grid (upstream)
$Q_{c,i,s,w,t}$	Reactive power injected by capacitor bank at node *i*
$\delta_{i,s,w,t}$	Unserved power at node *i*
P_k, Q_k, θ_k	Active and reactive power flows, and voltage angle difference of link k, respectively.
V_i, V_j	Voltage magnitudes at nodes *i* and *j*
$p_{k,s,w,t,l}, q_{k,s,w,t,l}$	Step variables used in linearization of quadratic flows

PL_k, QL_k	Active and reactive power losses, respectively
$P^{ch}_{es,i,s,w,t}, P^{dch}_{es,i,s,w,t}$	Power charged to and discharged from storage system
$D_{i,s,w,t}$, $Q_{i,s,w,t}$	Active and reactive power demand at node i
$PL_{ς,s,w,t}, QL_{ς,s,w,t}$	Active and reactive losses at substation ς
$I^{ch}_{es,i,s,w,t}, I^{dch}_{es,i,s,w,t}$	Charge-discharge indicator variables
$E_{es,i,s,w,t}$	Stored energy

d) Functions

$InvC^{DG}_t, MC^{DG}_t, EC^{DG}_t$	NPV investment/maintenance/expected energy cost of DGs, respectively
$InvC^{LN}_t, MC^{LN}_t$	NPV investment/maintenance cost of a distribution line
$InvC^{ES}_t, MC^{ES}_t, EC^{ES}_t$	NPV investment/maintenance/expected energy cost of an energy storage system, respectively
$InvC^{CAP}_t, MC^{Cap}_t$	NPV investment/maintenance cost of capacitor banks
EC^{SS}_t	Expected cost of energy purchased from upstream
$ENSC_t$	Expected cost of unserved power
$EmiC^{DG}_t$	Expected emission cost of power production using DG
$EmiC^{SS}_t$	Expected emission cost of purchased power
$EmiC^{N}_t, EmiC^{E}_t$	Expected emission cost of power production using new and existing DGs, respectively

REFERENCES

[1] Energy Information Administration. International Energy Outlook 2014. US Department of Energy; 2014.

[2] National Research Council. Advancing the Science of Climate Change. Washington, DC: The National Academies Press; 2010.

[3] Jordehi AR. Optimisation of electric distribution systems: A review. Renew Sustain Energy Rev 2015;51:1088–100. doi:10.1016/j.rser.2015.07.004.

[4] Soares T, Pereira F, Morais H, Vale Z. Cost allocation model for distribution networks considering high penetration of distributed energy resources. Electr Power Syst Res 2015;124:120–32. doi:10.1016/j.epsr.2015.03.008.

[5] Ray PK, Mohanty SR, Kishor N. Classification of Power Quality Disturbances Due to Environmental Characteristics in Distributed Generation System. IEEE Trans Sustain Energy 2013;4:302–13. doi:10.1109/TSTE.2012.2224678.

[6] Martinez IC, Chen C-Y, Teng J-H. Utilising energy storage systems to mitigate power system vulnerability. IET Gener Transm Distrib 2013;7:790–8. doi:10.1049/iet-gtd.2012.0694.

[7] Georgilakis PS, Hatziargyriou ND. Optimal Distributed Generation Placement in Power Distribution Networks: Models, Methods, and Future Research. IEEE Trans Power Syst 2013;28:3420–8. doi:10.1109/TPWRS.2012.2237043.

[8] Paliwal P, Patidar NP, Nema RK. Planning of grid integrated distributed generators: A review of technology, objectives and techniques. Renew Sustain Energy Rev 2014;40:557–70. doi:10.1016/j.rser.2014.07.200.

[9] Hung DQ, Mithulananthan N, Bansal RC. An optimal investment planning framework for multiple distributed generation units in industrial distribution systems. Appl Energy 2014;124:62–72. doi:10.1016/j.apenergy.2014.03.005.

[10] Abu-Mouti FS, El-Hawary ME. Heuristic curve-fitted technique for distributed generation optimisation in radial distribution feeder systems. IET Gener Transm Distrib 2011;5:172. doi:10.1049/iet-gtd.2009.0739.

[11] Pal BC, Jabr RA. Ordinal optimisation approach for locating and sizing of distributed generation. IET Gener Transm Distrib 2009;3:713–23. doi:10.1049/iet-gtd.2009.0019.

[12] Maciel RS, Rosa M, Miranda V, Padilha-Feltrin A. Multi-objective evolutionary particle swarm optimization in the assessment of the impact of distributed generation. Electr Power Syst Res 2012;89:100–8. doi:10.1016/j.epsr.2012.02.018.

[13] Vinothkumar K, Selvan MP. Fuzzy Embedded Genetic Algorithm Method for Distributed Generation Planning. Electr Power Compon Syst 2011;39:346–66. doi:10.1080/15325008.2010.528533.
[14] Ugranlı F, Karatepe E. Convergence of rule-of-thumb sizing and allocating rules of distributed generation in meshed power networks. Renew Sustain Energy Rev 2012;16:582–90. doi:10.1016/j.rser.2011.08.024.
[15] Murty VVSN, Kumar A. Optimal placement of DG in radial distribution systems based on new voltage stability index under load growth. Int J Electr Power Energy Syst 2015;69:246–56. doi:10.1016/j.ijepes.2014.12.080.
[16] Bagheri A, Monsef H, Lesani H. Integrated distribution network expansion planning incorporating distributed generation considering uncertainties, reliability, and operational conditions. Int J Electr Power Energy Syst 2015;73:56–70. doi:10.1016/j.ijepes.2015.03.010.
[17] Sheng W, Liu K, Liu Y, Meng X, Li Y. Optimal Placement and Sizing of Distributed Generation via an Improved Nondominated Sorting Genetic Algorithm II. IEEE Trans Power Deliv 2015;30:569–78. doi:10.1109/TPWRD.2014.2325938.
[18] Mena R, Hennebel M, Li Y-F, Ruiz C, Zio E. A risk-based simulation and multi-objective optimization framework for the integration of distributed renewable generation and storage. Renew Sustain Energy Rev 2014;37:778–93. doi:10.1016/j.rser.2014.05.046.
[19] Foster JD, Berry AM, Boland N, Waterer H. Comparison of Mixed-Integer Programming and Genetic Algorithm Methods for Distributed Generation Planning. IEEE Trans Power Syst 2014;29:833–43. doi:10.1109/TPWRS.2013.2287880.
[20] Ameli A, Bahrami S, Khazaeli F, Haghifam M-R. A Multiobjective Particle Swarm Optimization for Sizing and Placement of DGs from DG Owner's and Distribution Company's Viewpoints. IEEE Trans Power Deliv 2014;29:1831–40. doi:10.1109/TPWRD.2014.2300845.
[21] Wen S, Lan H, Fu Q, Yu DC, Zhang L. Economic Allocation for Energy Storage System Considering Wind Power Distribution. IEEE Trans Power Syst 2015;30:644–52. doi:10.1109/TPWRS.2014.2337936.
[22] Sedghi M, Aliakbar-Golkar M, Haghifam M-R. Distribution network expansion considering distributed generation and storage units using modified PSO algorithm. Int J Electr Power Energy Syst 2013;52:221–30. doi:10.1016/j.ijepes.2013.03.041.
[23] Saboori H, Hemmati R, Abbasi V. Multistage distribution network expansion planning considering the emerging energy storage systems. Energy Convers Manag 2015;105:938–45. doi:10.1016/j.enconman.2015.08.055.
[24] Aman MM, Jasmon GB, Bakar AHA, Mokhlis H. A new approach for optimum simultaneous multi-DG distributed generation Units placement and sizing based on maximization of system loadability using HPSO (hybrid particle swarm optimization) algorithm. Energy 2014;66:202–15. doi:10.1016/j.energy.2013.12.037.
[25] Rao RS, Ravindra K, Satish K, Narasimham SVL. Power Loss Minimization in Distribution System Using Network Reconfiguration in the Presence of Distributed Generation. IEEE Trans Power Syst 2013;28:317–25. doi:10.1109/TPWRS.2012.2197227.
[26] Nekooei K, Farsangi MM, Nezamabadi-Pour H, Lee KY. An Improved Multi-Objective Harmony Search for Optimal Placement of DGs in Distribution Systems. IEEE Trans Smart Grid 2013;4:557–67. doi:10.1109/TSG.2012.2237420.
[27] Sedighizadeh M, Esmaili M, Esmaeili M. Application of the hybrid Big Bang-Big Crunch algorithm to optimal reconfiguration and distributed generation power allocation in distribution systems. Energy 2014;76:920–30. doi:10.1016/j.energy.2014.09.004.
[28] Abdelaziz AY, Hegazy YG, El-Khattam W, Othman MM. Optimal allocation of stochastically dependent renewable energy based distributed generators in unbalanced distribution networks. Electr Power Syst Res 2015;119:34–44. doi:10.1016/j.epsr.2014.09.005.
[29] Othman MM, El-Khattam W, Hegazy YG, Abdelaziz AY. Optimal Placement and Sizing of Distributed Generators in Unbalanced Distribution Systems Using Supervised Big Bang-Big Crunch Method. IEEE Trans Power Syst 2015;30:911–9. doi:10.1109/TPWRS.2014.2331364.
[30] Rama Prabha D, Jayabarathi T, Umamageswari R, Saranya S. Optimal location and sizing of distributed generation unit using intelligent water drop algorithm. Sustain Energy Technol Assess 2015;11:106–13. doi:10.1016/j.seta.2015.07.003.

[31] Mohamed Imran A, Kowsalya M, Kothari DP. A novel integration technique for optimal network reconfiguration and distributed generation placement in power distribution networks. Int J Electr Power Energy Syst 2014;63:461–72. doi:10.1016/j.ijepes.2014.06.011.
[32] Singh AK, Parida SK. Allocation of distributed generation using proposed DMSP approach based on utility and customers aspects under deregulated environment. Int J Electr Power Energy Syst 2015;68:159–69. doi:10.1016/j.ijepes.2014.12.076.
[33] Al Abri RS, El-Saadany EF, Atwa YM. Optimal Placement and Sizing Method to Improve the Voltage Stability Margin in a Distribution System Using Distributed Generation. IEEE Trans Power Syst 2013;28:326–34. doi:10.1109/TPWRS.2012.2200049.
[34] Atwa YM, El-Saadany EF, Salama MMA, Seethapathy R. Optimal Renewable Resources Mix for Distribution System Energy Loss Minimization. IEEE Trans Power Syst 2010;25:360–70. doi:10.1109/TPWRS.2009.2030276.
[35] Yang Y, Zhang S, Xiao Y. An MILP (mixed integer linear programming) model for optimal design of district-scale distributed energy resource systems. Energy 2015. doi:10.1016/j.energy.2015.07.013.
[36] Montoya-Bueno S, Munoz JI, Contreras J. A Stochastic Investment Model for Renewable Generation in Distribution Systems. IEEE Trans Sustain Energy 2015;6:1466–74. doi:10.1109/TSTE.2015.2444438.
[37] Sfikas EE, Katsigiannis YA, Georgilakis PS. Simultaneous capacity optimization of distributed generation and storage in medium voltage microgrids. Int J Electr Power Energy Syst 2015;67:101–13. doi:10.1016/j.ijepes.2014.11.009.
[38] Mahmoud K, Yorino N, Ahmed A. Optimal Distributed Generation Allocation in Distribution Systems for Loss Minimization. IEEE Trans Power Syst 2015:1–10. doi:10.1109/TPWRS.2015.2418333.
[39] Vinothkumar K, Selvan MP. Hierarchical Agglomerative Clustering Algorithm method for distributed generation planning. Int J Electr Power Energy Syst 2014;56:259–69. doi:10.1016/j.ijepes.2013.11.021.
[40] Atwa YM, El-Saadany EF. Probabilistic approach for optimal allocation of wind-based distributed generation in distribution systems. IET Renew Power Gener 2011;5:79. doi:10.1049/iet-rpg.2009.0011.
[41] Murty VVS., Kumar A. Mesh distribution system analysis in presence of distributed generation with time varying load model. Int J Electr Power Energy Syst 2014;62:836–54. doi:10.1016/j.ijepes.2014.05.034.
[42] Blank L, Tarquin A. Engineering Economy. 7th ed. New York: McGraw-Hill Science/Engineering/Math; 2011.
[43] Munoz-Delgado G, Contreras J, Arroyo JM. Joint Expansion Planning of Distributed Generation and Distribution Networks. IEEE Trans Power Syst 2015;30:2579–90. doi:10.1109/TPWRS.2014.2364960.
[44] Phonrattanasak P. Optimal placement of DG using multiobjective particle swarm optimization. 2010 2nd Int. Conf. Mech. Electr. Technol. ICMET, 2010, p. 342–6. doi:10.1109/ICMET.2010.5598377.
[45] Zhang H, Heydt GT, Vittal V, Quintero J. An Improved Network Model for Transmission Expansion Planning Considering Reactive Power and Network Losses. IEEE Trans Power Syst 2013;28:3471–9. doi:10.1109/TPWRS.2013.2250318.
[46] Vielma JP, Ahmed S, Nemhauser G. Mixed-Integer Models for Nonseparable Piecewise-Linear Optimization: Unifying Framework and Extensions. Oper Res 2009;58:303–15. doi:10.1287/opre.1090.0721.
[47] Williams HP. Model Building in Mathematical Programming. 4th ed. Wiley; 1999.
[48] Romero-Ramos E, Riquelme-Santos J, Reyes J. A simpler and exact mathematical model for the computation of the minimal power losses tree. Electr Power Syst Res 2010;80:562–71. doi:10.1016/j.epsr.2009.10.016.
[49] Lavorato M, Franco JF, Rider MJ, Romero R. Imposing Radiality Constraints in Distribution System Optimization Problems. IEEE Trans Power Syst 2012;27:172–80. doi:10.1109/TPWRS.2011.2161349.

[50] Zhang J, Yuan X, Yuan Y. A novel genetic algorithm based on all spanning trees of undirected graph for distribution network reconfiguration. J Mod Power Syst Clean Energy 2014;2:143–9. doi:10.1007/s40565-014-0056-0.
[51] Ahmadi H, Martí JR. Mathematical representation of radiality constraint in distribution system reconfiguration problem. Int J Electr Power Energy Syst 2015;64:293–9. doi:10.1016/j.ijepes.2014.06.076.
[52] Georgilakis PS, Hatziargyriou ND. A review of power distribution planning in the modern power systems era: Models, methods and future research. Electr Power Syst Res 2015;121:89–100. doi:10.1016/j.epsr.2014.12.010.
[53] Sinden G. Characteristics of the UK wind resource: Long-term patterns and relationship to electricity demand. Energy Policy 2007;35:112–27. doi:10.1016/j.enpol.2005.10.003.
[54] Subhadarshi S. Minding the Ps and Qs_ Real and reactive power assessment of hybrid energy conversion systems with wind and solar resources n.d. http://lib.dr.iastate.edu/cgi/viewcontent.cgi?article=4236&context=etd (accessed August 20, 2015).
[55] Li YZ, Wu QH, Li MS, Zhan JP. Mean-variance model for power system economic dispatch with wind power integrated. Energy 2014;72:510–20. doi:10.1016/j.energy.2014.05.073.
[56] Zhao M, Chen Z, Blaabjerg F. Probabilistic capacity of a grid connected wind farm based on optimization method. Renew Energy 2006;31:2171–87. doi:10.1016/j.renene.2005.10.010.
[57] Aien M, Rashidinejad M, Fotuhi-Firuzabad M. On possibilistic and probabilistic uncertainty assessment of power flow problem: A review and a new approach. Renew Sustain Energy Rev 2014;37:883–95. doi:10.1016/j.rser.2014.05.063.
[58] Wang M, Zhong J. Islanding of systems of distributed generation using optimization methodology. 2012 IEEE Power Energy Soc. Gen. Meet., 2012, p. 1–7. doi:10.1109/PESGM.2012.6345009.
[59] Fitiwi DZ, Olmos L, Rivier M, Cuadra F de. Finding a representative network losses model for large-scale transmission expansion planning with renewable energy sources. Energy n.d. doi:in press.
[60] Ellis A, Nelson R, Von Engeln E, Walling R, MacDowell J, Casey L, et al. Reactive power performance requirements for wind and solar plants. 2012 IEEE Power Energy Soc. Gen. Meet., 2012, p. 1–8. doi:10.1109/PESGM.2012.6345568.